ORIGINAL ARTICLE

Investigation of RC structure damages after February 6, 2023, Kahramanmaraş earthquake in the Hatay region

Talha Polat Doğan[1] · Hüseyin Kalkan[1] · Ömer Aldemir[1] · Murat Ayhan[1] ·
Meryem Böcek[1] · Özgür Anıl[1]

Abstract

From a tectonic perspective, Türkiye is a geographical region known for its high seismic activity, with some of the most active faults in the world. On February 6, 2023, two consecutive earthquakes with magnitudes of Mw 7.7 and Mw 7.6 struck Kahramanmaraş within a remarkably short time span of 9 h. This event stands out as a rare and unprecedented tectonic occurrence in terms of seismicity and tectonic activity over the past 100 years. The impact of these two major earthquakes on the region's reinforced concrete structures was significant, resulting in severe damage and the collapse of numerous buildings. It is of utmost importance to investigate and examine the design flaws and underlying factors that contributed to the damage observed in the reinforced concrete structures affected by these earthquakes. Such research will not only contribute to the improvement of structural design, seismic regulations, and quality control measures during construction but also enhance our understanding of earthquake engineering. In this study, an in-depth field investigation was conducted on reinforced concrete structures in Hatay, one of the regions most affected by the Kahramanmaraş earthquakes. The damages occurring in the buildings were documented through a detailed field survey and analyzed. A total of 540 reinforced concrete structures in the Hatay region were extensively examined, and the damages that occurred in these structures were photographed and interpreted to understand their underlying causes. Subsequently, based on the findings from the field investigation, a structural model was designed that incorporated the most significant design and construction errors responsible for the damages observed in the 540 examined structures. The devised model was subjected to static push-over analysis and nonlinear dynamic analysis using the SAP2000 finite element software, and the results obtained were interpreted.

Keywords Kahramanmaraş earthquakes · Field ınvestigations · Static push-over analysis · Nonlinear time history analysis · RC structure

✉ Özgür Anıl
    oanil@gazi.edu.tr

1   Civil Engineering Department, Gazi University, Ankara, Türkiye

1 Introductıon

The examination of the affected building stock in the aftermath of major earthquakes and the interpretation of the damages incurred on the structures contribute significantly to the seismic engineering literature. Understanding how structures are affected by real and major earthquakes, the types of damages they experience as a result, the underlying causes of damage mechanisms, and the identification of design errors that contribute to these damages are highly significant topics. These research areas provide a vital foundation for numerous scientific and academic research endeavors. They enable the development of solutions to prevent the recurrence of these design and construction errors and facilitate the advancement of seismic codes. They also underline the importance of construction workers' training and skills. Through extensive scientific and academic research, these areas play a significant role in shaping the field and ultimately contribute to the improvement of seismic regulations and guidelines. These are pivotal subjects that hold immense importance in the field of earthquake engineering. Detailed field investigations that focus on the damages to the building stock, the design and construction errors responsible for these damages are of paramount importance and make significant contributions to the seismic engineering literature. These investigations provide valuable insights for proposing solutions and recommendations to prevent the recurrence of similar construction errors. Moreover, they have played a vital role in the revision of seismic codes and regulations in many countries, as well as inspiring further research endeavours in the field of earthquake engineering.

Türkiye is located in a tectonically active region characterized by frequent occurrence of large-scale earthquakes. Consequently, observational field studies conducted after major earthquakes contribute significantly to the earthquake engineering literature. The earthquakes that occurred on February 6, 2023, in Kahramanmaraş, with magnitudes of Mw 7.7 and Mw 7.6, and only a short time difference between them (9 h), have made notable contributions to this literature. Investigations have indicated that the occurrence of two major earthquakes with such a short time difference is a rare and infrequent tectonic event within the past 100 years. Following this unique and rare tectonic event, field surveys in the affected region are deemed essential for examining the damages incurred in the building stock, interpreting the underlying design errors that led to these damages, and providing significant insights to the existing literature. Hence, a comprehensive field study has been planned to investigate the reinforced concrete structures in Hatay, which is one of the regions most affected by the Kahramanmaraş earthquakes. A total of 540 reinforced concrete structures have been meticulously examined, and the damages observed have been photographed and categorized. The design errors and underlying causes behind the damages observed in the examined reinforced concrete structures were interpreted and analyzed. In the second part of the study, the most commonly encountered design errors that lead to damages in reinforced concrete structures were identified. A structural model incorporating these errors was designed, and analysis was performed using the SAP2000 finite element analysis program. RC structure models underwent static push-over analysis and nonlinear dynamic analysis within a defined time frame to assess its seismic performance. The obtained results were then compared with the real observational findings from the field studies.

After past devastating earthquakes, various researchers have conducted academic observations. These earthquakes serve as life-size scale experiments for the civil engineering literature. The findings from these earthquakes are crucial for improving future

construction practices (Ates et al. 2013; Demirel et al. 2022; Doğangün 2004; Yakut, et al. 2021). Extensive damage assessment studies have been conducted following the earthquakes in Marmara, Bingöl, Elazığ, Van, İzmir, and Kahramanmaraş over the past 20 years. These studies have examined the main causes and consequences of structural and non-structural damage observed in reinforced concrete structures (Doğan et al. 2021; Yüksel 2008). In the literature, one of the main causes of structural damage is attributed to the presence of structural irregularities specified in the building codes and regulations (Ates et al. 2013; Demirel et al. 2022; Kirac et al. 2011). According to the research conducted by Kirac et al. (2011), it was observed that 82% of the 788 examined buildings have weak storey irregularities. Similarly, in a field survey conducted by Demirel et al. (2022) which covered 140 buildings, it was reported that 86% of the structures had soft storey irregularities, 36% had plan irregularities, 71% had overhangs, and 29% had short column issues. In addition, some studies have indicated that diagonal or discontinuous structural system geometries can also contribute to earthquake damage (Doğan et al. 2021). Among the main causes of the encountered earthquake damage are deficiencies in the structural system, as well as inadequate material quality and poor reinforcement details. Post-earthquake field investigations have revealed that the concrete compressive strength of heavily damaged structures is approximately 10 MPa (Demirel et al. 2022; Doğangün 2004; Çağatay 2005; Kaplan et al. 2004). Additionally, bond slip-induced damages have been discussed in structural elements where longitudinal reinforcement is not adequately bonded (Doğangün 2004; Inel and Ozmen 2006). Another commonly encountered issue among reinforcement defects is the failure of stirrups to perform their intended confinement function due to the application of 90-degree hooks. Various studies have stated that structural damage occurs frequently due to the lack of confinement reinforcement at column-beam ends and joint regions in the literature (Yakut, et al. 2021; Arslan and Korkmaz 2007; Bayraktar et al. 2013; Sezen et al. 2003). The errors outlined, such as insufficient material strength and inadequate confinement reinforcement, do not arise from designer or regulatory oversight, but rather from subpar manufacturing quality.

In studies conducted based on field investigations, it has been reported that some buildings, despite receiving engineering services during the design process, suffered damage or collapsed after earthquakes. Researchers have attributed this situation to the lack of adequate engineering services and supervision during the construction phase (Yüksel 2008; Arslan and Korkmaz 2007; Bayraktar et al. 2013). Post-earthquake seismic vulnerability assessments of buildings consist of three stages: (1) rapid visual screening (RVS), (2) preliminary vulnerability assessment (PVA), and (3) detailed vulnerability assessment (DVA) (Doğan et al. 2021; Bektaş and Kegyes-Brassai 2023). The RVS method is a practical approach that can be quickly applied post-earthquake, relying on visual inspection for assessment (Bhalkikar and Kumar 2021). The PVA methods, while not relying on complex and time-consuming structural analyses, still require field data obtained from site inspections along with measurements and orientations of structural elements, material properties, and building plans to conduct the evaluation (Bhalkikar and Kumar 2021; Achs and Adam 2012; Haryanto et al. 2020; Nanda and Majhi 2013; Yakut 2004). Collecting the mentioned data contradicts the urgent need to complete the assessment of the affected building stock after an earthquake. As a result, the most common and prioritized evaluation method used after an earthquake is RVS (Yakut 2004). After the earthquakes in Pazarcık and Elbistan on February 6, 2023, and Hatay Defne and Samandağ on February 20, 2023, RVS activities were carried out rapidly under the coordination of the Republic of Türkiye's governmental institutions and organizations.

There are several RVS methods that enable the rapid preliminary assessment of large building stocks. Among the methods used in Türkiye are RBTE-2019 (Principles for Identifying Risky Buildings 2012) and The Modified Post-Earthquake Damage Assessment Methodology (Ilki et al. 2021), which is used for the Turkish Catastrophe Insurance Pool. Additionally, FEMA P-154 (FEMA-154 2017) prepared by the United States Federal Emergency Management Agency can also be mentioned among these methods. Although there are widely accepted and traditionally used RVS methods, these methods need to be confirmed with DVA methods in the later stages. Harirchian and Lahmer (2020), in their study examining the evaluation results on reinforced concrete (RC) structures using American (FEMA-154 2017), Turkish (Earthquake Master Plan for Istanbul (EMPI)) (Ansal et al. 2003), and Tesfamariam and Saatcioglu (2008) RVS methods for the Bingöl and Düzce regions in Türkiye, demonstrated that the accuracy levels of RVS methods can be misleading. After the 1999 Düzce earthquake, a study of 484 structures revealed that the damage levels were accurately classified as 17.1% with the American RVS method and 28.3% with the Turkish RVS method, reflecting the actual condition. Following the 2003 Bingöl earthquake, the examination of 28 structures resulted in accuracies of 10.7% with the American RVS method, 17.8% with the Turkish RVS method, and 60.7% with the Tesfamariam and Saatcioglu (2008) method. In the same study, using the proposed hierarchical type-2 fuzzy logic model method, accuracies of 62.2% for the Düzce region and 64.3% for the Bingöl region were achieved.

Due to the concerning levels of accuracy in damage assessment, it is essential for the findings obtained through RVS methods to be confirmed by DVA methods as well (Arslan and Korkmaz 2007; Erdil and Ceylan 2019; Tapan et al. 2013). In this study, pushover analysis and nonlinear time history analysis were conducted to test the validity of the Rapid Visual Screening (RVS) assessments made by the authors based on field observations following the earthquakes that occurred on February 6, 2023, in Pazarcık and Elbistan, and on February 20, 2023, in Hatay Defne and Samandağ. This allowed for the evaluation of the consistency between the findings obtained from field observations and the comprehensive analysis results.

2 Earthquakes ın Türkiye and the Hatay regıon

Türkiye is situated in the centre of the Alp-Himalayan orogenic belt, which is one of the most active regions for seismic activities in the world (McKenzie 1972). The seismic belt in which Türkiye is located has witnessed numerous destructive earthquakes throughout history. Within this belt, there are several tectonic structures, as shown in Fig. 1, such as the strike-slip faults (North Anatolian Fault Zone and East Anatolian Fault Zone), the continental collision zone (Bitlis-Zagros Fault Thrust Zone), and the continental rift zone (Aegean Graben Systems and the Marmara Sea) (McKenzie 1972). The Anatolian Plate is bounded by the Eurasian Plate to the north, the Arabian Plate to the southeast, and the African Plate to the south. Due to the movement of the Arabian Plate towards the Eurasian Plate, the Anatolian Plate is being pushed westward (McKenzie 1978). As a result of these movements, the Anatolian Plate has encountered two major fault systems: the right-lateral strike-slip North Anatolian Fault Zone (NAFZ) and the left-lateral strike-slip East Anatolian Fault Zone (EAFZ). The NAFZ begins from Bingöl-Karlıova, moves in a northwest direction, crosses the Marmara Sea, and extends all the way to Greece via Çanakkale. On the other hand, the EAFZ starts from
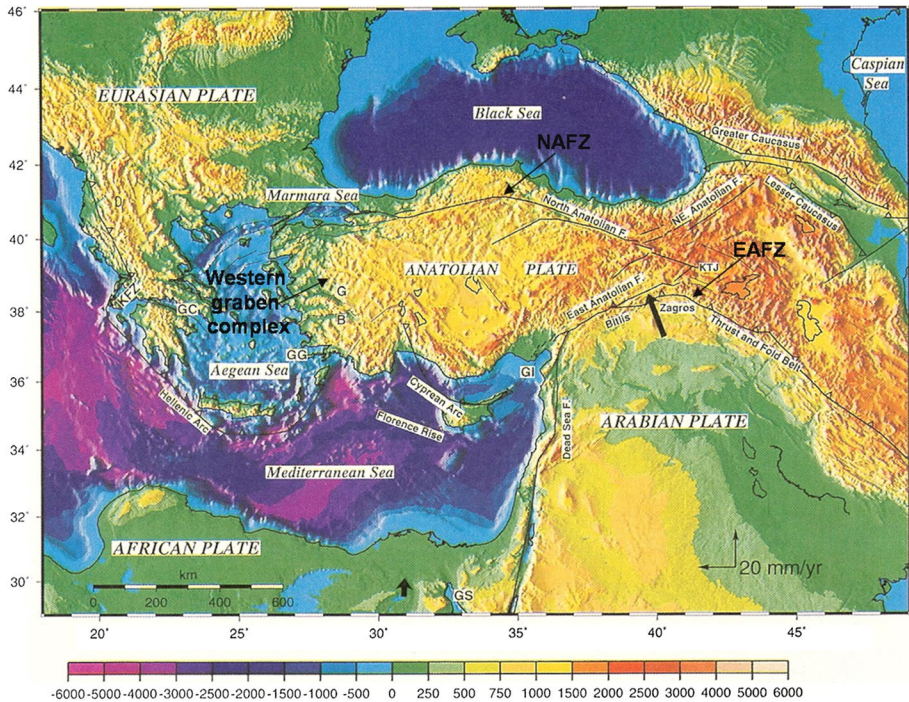
Fig. 1 Tectonic, topographic and bathymetric map of the Anatolian region (McKenzie 1972, 1978)

the same region, but moves southwest through Kahramanmaraş and reaches Antakya, where it intersects with the Dead Sea Fault Zone (Şengör et al. 1985; Barka and Kadinsky-Cade 1988).

The historical earthquakes that have occurred along the East Anatolian Fault Zone are as follows: Antakya 115–526, Maraş (Pazarcık) 1114–1513, Maraş 1822, Elazığ 1866, Antakya 1872, Elazığ 1874–1875 (Gezin-Sivrice), Malatya 1893–1905 (Çelikhan-Pötürge), Bingöl 1945–1971 (Karlıova), Malatya 1986 (Sürgü), Adana 1998 (Ceyhan), Elazığ 2020 (Sivrice) (Şaroğlu et al. 1987; Demirtaş and Yılmaz 1996; Ateş and Bayülke 1977). The earthquakes that occurred between the eighteenth and twentieth centuries on the Eastern Anatolian Fault Zone, causing surface ruptures, took place in the Erkenek Segment, Gölbaşı Segment, Amonos Segment, Yesemek Segment, and Adana Segment. However, there has been no seismic activity between Gölbaşı and Türkoğlu for over 500 years (Demirtaş and Yılmaz 1996; Ambraseys and Jackson 1998; Arpat 1971; Arpat and Şaroğlu 1972; Duman and Emre 2013; Seymen and Aydin 1972).

On February 6, 2023, at 04:17 (Türkiye local time), a 7.7 (Mw) magnitude earthquake occurred on the Narlı segment of the Eastern Anatolian Fault Zone (EAFZ), known as the Pazarcık earthquake. Another earthquake with a magnitude of 7.6 Mw, known as the Elbistan earthquake, took place on the Çardaklı fault at 13:24. As a result of these earthquakes, the seismic gap between Adıyaman Gölbaşı and Kahramanmaraş Türkoğlu was closed through fault rupture. Following these earthquakes, thousands of aftershocks, the largest of which had a magnitude of 6.4 Mw, occurred in the region as shown in Fig. 2 (DEMP 2018). On February 20, 2023, earthquakes with magnitudes of
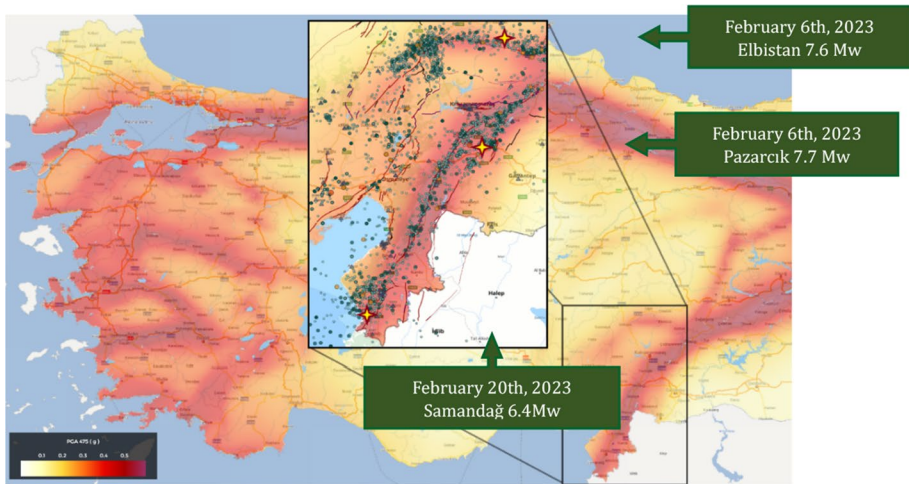
Fig. 2 Earthquake hazard map of Türkiye with 6 February and 20 February earthquakes (DEMP 2018)

6.4 Mw and 5.8 Mw occurred in the Hatay Defne and Samandağ regions. These earthquakes were triggered by the earlier earthquakes in Kahramanmaraş.

Following these earthquakes, detailed field inspections were carried out in the districts of Antakya and Defne in Hatay. It was observed that the extent of destruction and the number of heavily damaged buildings were quite high, depending on the magnitude of the earthquakes. The measured acceleration values in the affected region, considering the local site classes according to Eurocode 8 (EC8) and the Turkish Building Earthquake Code 2018 (TBEC2018), are presented in Table 1 (Standard 2005; TBEC2018 2018). In the region where field observations were conducted, the acceleration values obtained from the Elbistan earthquake remained around 2.5–2.6 Gal, so these earthquake records were not used for both the studied buildings and the numerical analyses conducted within this study. The acceleration and design spectrum comparisons for the stations located in the region marked in Fig. 3, which correspond to the Pazarcık and Samandağ earthquakes, can be seen in Fig. 4. As seen in Fig. 4, it has been observed that the predicted accelerations in the range of 0.8–1.5 s to 2–4 s significantly exceeded (100–200%) in the 3125 Pazarcık records. For the 3125 Samandağ records, design accelerations have been exceeded, especially in the constant acceleration region (180%).

Table 1 Event properties obtained from the stations near defne district (DEMP 2018)

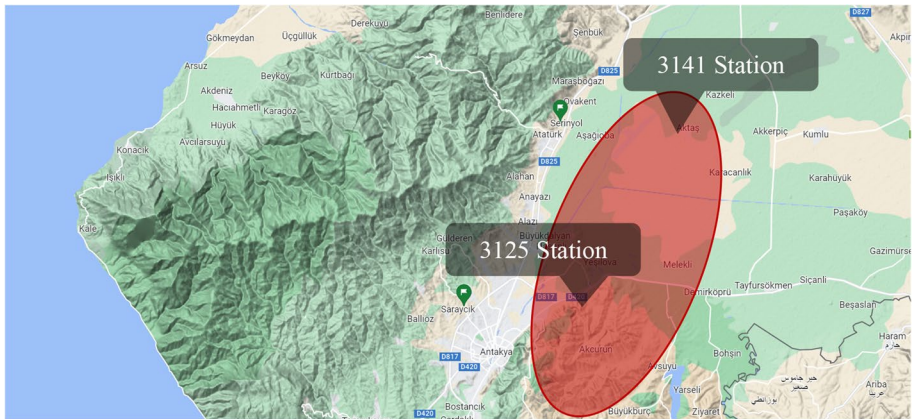| Event	Magnitude (Mw)	Hypocentral distance (km)	Station code	Station distance to epicentre (km)	Vs30 (m/s)	Site class (EC8/TBEC2018)	PGA (g)
Pazarcık	7.7	8.6	3125	142	448	B/C	1.143
			3141	125	338	C/D	0.979
Elbistan	7.6	7	3125	228	448	B/C	0.025
			3141	211	338	C/D	0.026
Samandağ	6.4	21.7	3125	25	448	B/C	0.79
			3141	41	338	C/D	0.395

Fig. 3 Investigated area and locations of the stations

Similarly, for the 3141 Pazarcık records, design accelerations have been exceeded in both the constant acceleration region and the 1.5–3 s range (230%). However, for the 3141 Samandağ records, values close to the expected design accelerations have been observed for all period values. Due to the exceeded design accelerations, more damage has been observed in buildings within these period ranges. Considering this situation, the building models designed in this study have been designed to have an effective period of ~1 s. The soil parameters of stations 3125 and 3141 were found to be compatible with the site classes of the examined buildings; therefore, acceleration data were obtained from these two stations. Since the analysis models were designed to represent the building stock in the region, input records were used in the analyses without any correction or scaling applied.

When comparing the response spectra obtained from stations 3125 and 3141 near the Defne district where field inspections were conducted, it can be observed that the Pazarcık earthquake, particularly based on the data from station 3141 (Fig. 4b), reached acceleration values of 1 g up to a period of 2.0 s. Additionally, acceleration values between 2.5 and 3 g were recorded for period values up to that point. Similarly, for station 3125, the E–W component of the Pazarcık earthquake (Fig. 4a) did not fall below 1 g until a period of 1.0 s. The occurrence of such magnitudes of acceleration supports the observation of extensive damage and a high number of heavily damaged buildings during the earthquake zone visit prior to the Samandağ earthquake. Field visits conducted after the Samandağ earthquake also revealed an increase in the total number of collapsed buildings compared to the previous observations, with lightly to moderately damaged buildings transitioning to the level of heavily damaged buildings. This is the result of the Samandağ earthquake, which, although producing lower energy, affected buildings with accelerations above 0.5 g, particularly those that were already in a plastic state after the Pazarcık earthquake or had surpassed the elastic limit.

3 Fıeld observatıons

On February 6, 2023, two earthquakes with magnitudes of 7.7 and 7.6 (Mw), centred in Kahramanmaraş, occurred within a span of 10 h. According to official data, these earthquakes resulted in the collapse or severe damage of over 60,000 buildings. These
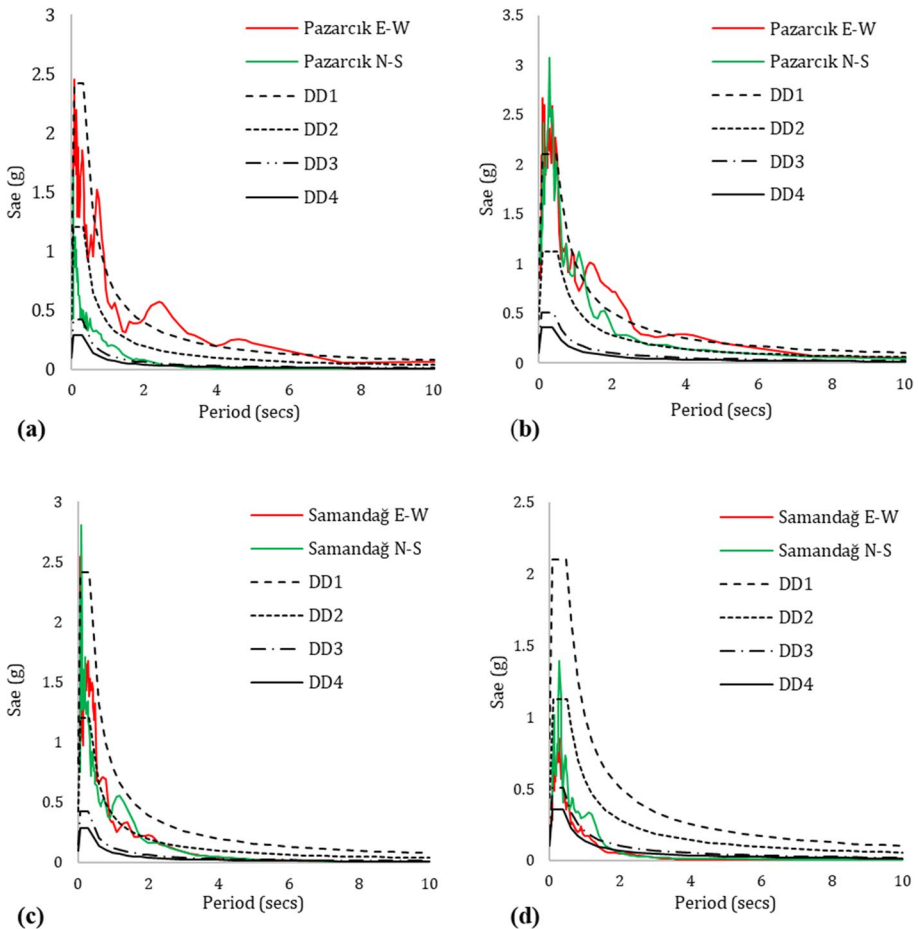
Fig. 4 Acceleration spectrums **a** Pazarcık event station code 3125, **b** Pazarcık event station code 3141, **c** Samandağ event station code 3125, **d** Samandağ event station code 3141 (DEMP 2018)

earthquakes, which affected approximately 100,000 square kilometres and paralyzed 10 provinces with a population of over 15 million, were followed by another earthquake centred in Samandağ, Hatay, on February 20. Field observations were conducted in Hatay, where the death toll reached the highest number of fatalities, with 22,000 deaths, in earthquakes that affected a total of 11 provinces, where the total number of casualties exceeded 50,000. Two visits were made to the region with a three-week interval, during which a total of 540 buildings were inspected. The inspections focused on buildings that were still standing and had only reinforced concrete (RC) structural systems. The number of buildings damaged due to ground deformations in the examined region is quite low, so such damages or collapses have not been included in this study. The collapse patterns and causes of the collapsed buildings were examined, but data specifically related to these buildings were not collected. As a result of these inspections, the current condition of the post-earthquake building stock in the visited area is presented in Table 2. The teams responsible for post-earthquake disaster management and risk assessments have conducted field

investigations using the assessment method proposed by Ilki et al. (2021). According to this method, a building is classified as heavily damaged if it has at least three vertical RC structural elements with concrete cover spalling, or if it has at least one vertical RC structural element with buckling of reinforcement, core crushing, and residual displacement. In such cases, heavily damaged buildings are considered to require demolition. However, the results obtained from field research suggest that this method is economically rigid and engineering-wise conservative. The field investigations conducted by the authors classified the damage levels of buildings by interpreting the locations and extent of damage, without strictly adhering to this method.

The observations conducted categorized seismic damages in buildings into structural and non-structural damages, as shown in Fig. 5. The buildings in the examined areas were generally constructed in compliance with modern earthquake regulations. Therefore, non-structural damages were minimal or nonexistent, and these types of damages were excluded from the scope of this article.

In the field observations conducted immediately after the February 6 earthquakes, numerous buildings were found to be completely or partially collapsed. Among these buildings, older structures, generally over 20 years old, were particularly affected by the failure of columns due to the strong beam-weak column design and shear damage at beam-column joints, which played a significant role in their collapse. Notwithstanding the presence of design provisions addressing beam-column connections in the seismic regulations of 1975 and 1998, substandard construction quality and inadequate supervision have resulted in structural damage to buildings. Furthermore, the seismic regulations enacted in 1998 introduced a design methodology centered on strong column-weak beam. Additionally, as shown in Fig. 6, the use of low-strength reinforcement bars, 135-degree hookless stirrups, and the use of concrete mixes containing irregularly graded sand and sea sand with salt and organic matter as aggregates were frequently observed. On the other hand, in buildings that were 20 years or newer, collapses occurred due to the soft story and weak story irregularities, resulting in the type of collapse exemplified in Fig. 7, where ground-floor columns failed.

The observed damages in the examined buildings in the disaster-stricken area, as indicated in Table 2, suggest that they generally exhibited ductile behaviour. Among the majority of the intact buildings, flexural damages in beams, as shown in Fig. 8, were frequently observed. However, even in buildings that could be considered "new" shear damages in beams were frequently observed. This can be attributed to architectural reasons and the preference for short beams and diagonal axes in the structural system design, as well as the inadequate use of secondary beams and insufficient confinement, as illustrated in Fig. 9. As a result, shear damages in beams were often observed, even in buildings expected to demonstrate ductile behaviour.

Table 2 Damage stage distributions of the examined building stock

Damage stage	Number of buildings
No damage	33
Minor damage	123
Moderate damage	145
Major damage	210
Requiring demolition	29
Total	**540**

a) Flexural damage on Beams   **b)** Shear Damage on Beams **c)** Beam-Column Joint Damage

d) Flexural damage on Columns **e)** Shear Damage on Columns **f)** Short Column Damage

g) Flexural damage on RC Walls   **h)** Shear Damage on RC Walls
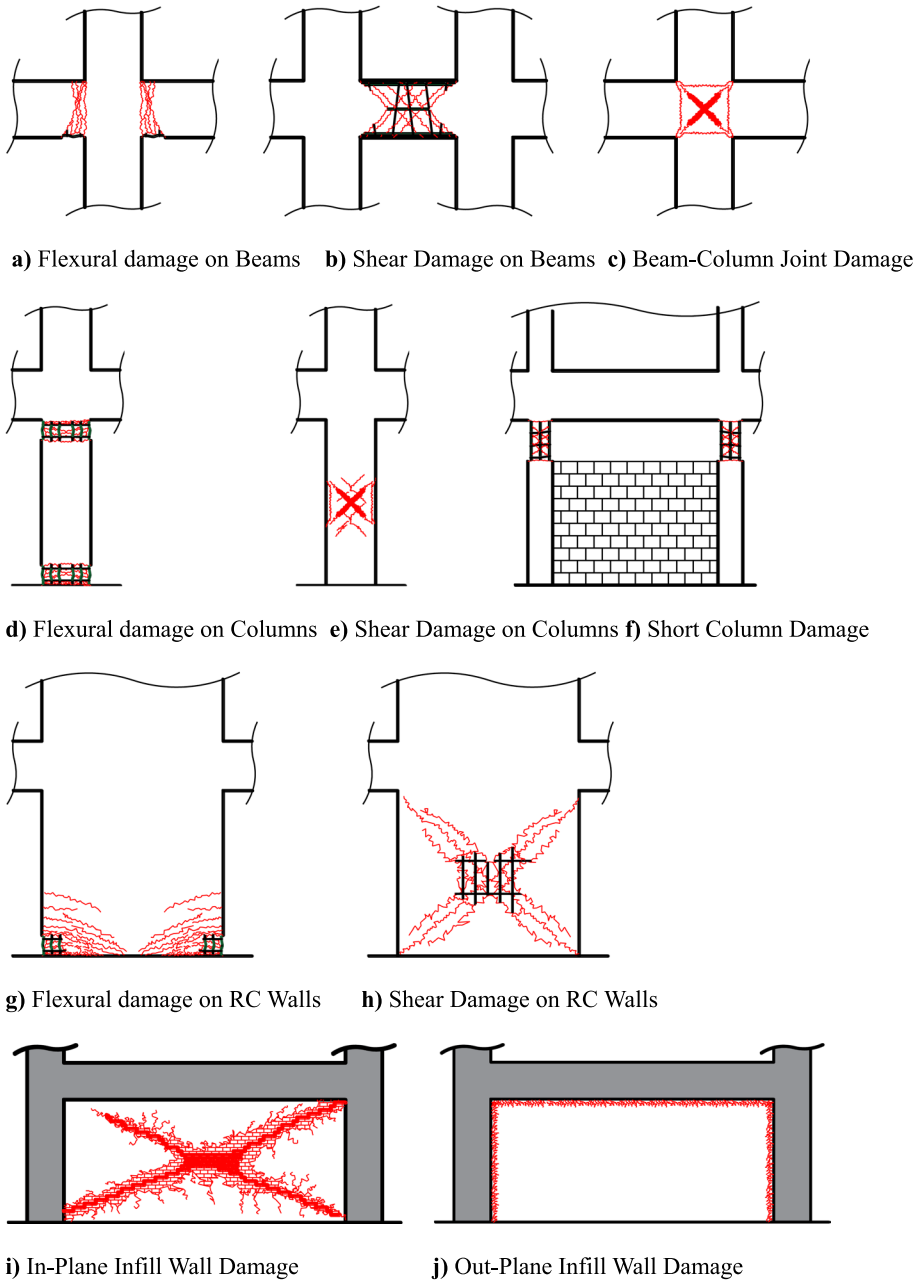
i) In-Plane Infill Wall Damage   **j)** Out-Plane Infill Wall Damage

Fig. 5 Structural and non-structural damages

Especially in buildings that have suffered severe damage but have not collapsed partially or completely, plastic hinges have formed at the lower ends of the ground floor columns and sometimes at both ends, as shown in Fig. 10, transitioning the structure
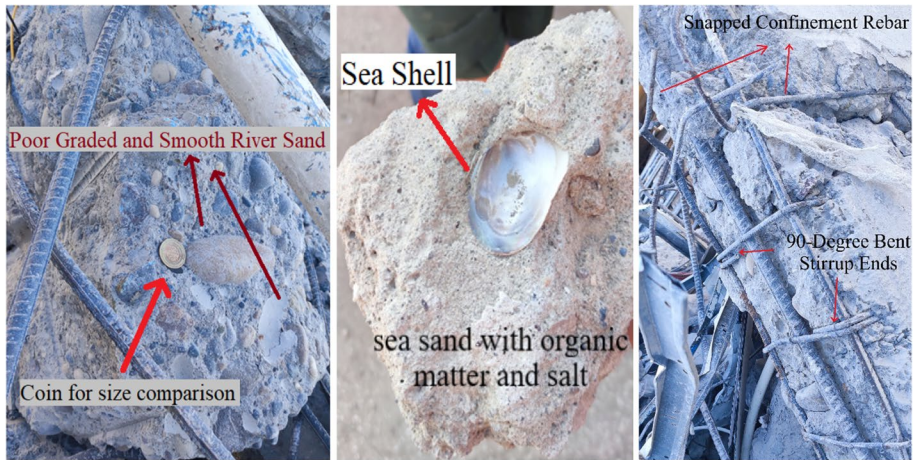
Fig. 6 Material based observed material and manufacturing defects

into a mechanism state. These types of damages are observed in buildings that can be considered relatively new.

Unlike the bending-damaged columns, in short columns where there is a sufficient amount of longitudinal and shear reinforcement against bending effects, sudden and brittle failure known as short column failure occurs due to errors based on architectural or structural design. Among the examined buildings, in the buildings where this type of damage, as shown in Fig. 11, was observed, almost no other types of damage were found. However, the shear-damaged columns shown in Fig. 12 have only suffered shear damage due to insufficient confinement. These brittle shear failures are generally observed in the ground floors of buildings. Although these buildings have been able to ensure life safety despite having these errors, the reasons for the collapse of the buildings that have collapsed are also related to these damages.

When considering the overall structural systems of the examined buildings, it is observed that reinforced concrete shear walls experience bending or shear damage according to their placement in the floor plans. The provided Fig. 13 illustrates shear walls with flexural damage, which are generally located on the exterior axes of the buildings' floor plans. On the other hand, Fig. 14 displays shear walls with shear damage, typically found on the interior axes of the RC walls. In all damaged RC walls, it has been determined that the confinement reinforcement application was insufficient.

During the field visits, it was observed that the collapsed buildings typically experienced damage at the column-beam connection regions, causing the columns to detach from the frame. The damage in this region was due to shear forces, resulting in brittle failure and the formation of a hinge at the node, leading to the collapse of the building as it transitioned into a mechanism state. In the undamaged buildings as well, damage was observed at the connection regions, as shown in Fig. 15. The connection region damage was predominantly found on the exterior axes of the buildings. In reinforced concrete structures, this region plays a significant role in achieving the intended performance of the building. Among the examined buildings, there is a considerable number of structures that have adequate confinement reinforcement in columns and beams

Fig. 7 Tilted or partially collapsed buildings

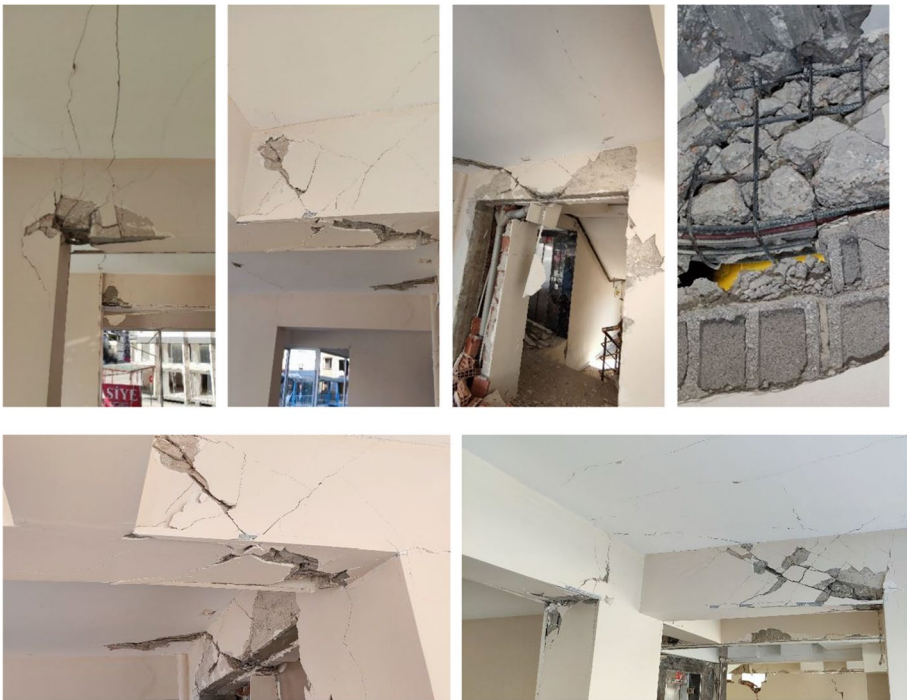**Fig. 8** Flexural damages on beams

Fig. 9 Shear damages on beams

according to TSC2007 and TBEC2018, but lack sufficient confinement at the column-beam connections, resulting in shear damage in these regions.

Frequently overlooked in structural system designs, but significantly contributing to the transfer of lateral forces during an earthquake, infill walls have also been observed to sustain damage. Figure 16 illustrates infill walls damaged under in-plane seismic loads. In the earthquake-affected region, it was often observed that during the construction of infill walls, they were not connected to the vertical load-bearing elements on both sides,

Fig. 10 Flexural damage on columns

Fig. 11 Short column damage

and no compression was applied to the wall under the beam or slab above it, leading to premature failure, out-of-plane damage, or toppling. Figure 17 provides an example of out-of-plane damage illustrating this situation.

Field observations revealed various data from the examined buildings, including structural system deficiencies, types of damage, causes of damage formation, and collapse mechanisms of the collapsed buildings. To enhance the study, these data were incorporated into a numerical analysis model, and the analysis results were used to support the findings obtained from the field observations.

Fig. 12 Shear damage on columns

4 Analysıs study

Approximately 70% of the 540 buildings examined in the disaster-stricken area were constructed within the last 20 years. This indicates that the majority of these structures were built in accordance with modern design codes. However, it was observed that attention was not paid to the details mandated by the codes in the damaged elements under investigation. Additionally, there was a lack of measures taken against irregularities specified in the codes, and architectural considerations led to the inclusion of short beams or diagonal axes in the structural system, disregarding engineering foresight. As a result, elements that were resistant to bending and shear effects but susceptible to secondary effects were frequently encountered.

The structural irregularities and construction deficiencies frequently observed in the examined buildings have been meticulously considered during the design phase of the analysis models. The most notable deficiency observed during field observations is the insufficient reinforcement of structural elements. Even in buildings designed in compliance with the TSC2007 and TBEC2018 codes, which prioritize ductile behaviour, the adequate spacing of reinforcement ties in confinement zones is often not

Fig. 13 Flexural damage on RC walls

Fig. 14 Shear damage on RC walls

observed (TBEC2018 2018; Turkish Earthquake Code 2007). Furthermore, according to TSC2007 and TBEC2018, the placement of the first stirrup at the ends of columns and beams should be at a distance of 50 mm from the beam-column joint. However, when examining the flexural damage in beam ends (Figs. 8 and 9), it has been observed that the first stirrup is approximately 100–150 mm away from the column, leading to brittle cracks and causing the longitudinal reinforcement to buckle due to hysteresis loading.

Fig.15 Shear damage on beam-column joint

Furthermore, another important observation in the examined buildings was the frequent occurrence of short-span beams. These elements had excessive reinforcement for moment capacity, but inadequate stirrup reinforcement, resulting in severe shear damage and even failure of the stirrups. In Türkiye, despite the definitive provisions regarding the flexural and shear strengths of relevant elements in the TS500 standard (Requirements for Design and Construction of Reinforced Concrete Structures TS500 2000),

Fig. 16 In-plane ınfill wall damages

Fig. 17 Out-plane ınfill wall damages

which is the standard used for the design of reinforced concrete structures, instances of such damages have been encountered even in new buildings due to designer and manufacturing errors. Contrary to the confinement regulations given by the seismic codes, in columns, the excessive distance between the first stirrup at the element ends and the column-beam joint, as well as the insufficient stirrup spacing in the confinement region, caused the columns to experience earlier and more extensive damage compared to the beams in the structure. Another common damage observed in buildings due to insufficient confinement was observed at column-beam joints. This type of damage, resulting from inadequate stirrup reinforcement, was prevalent in the majority of the examined buildings. In addition to these findings, it was observed that in buildings where the stirrup reinforcement was adequately spaced, the hooks of the stirrups were bent at 90° instead of 135°, leading to the opening and ineffective confinement of the existing

stirrups in these regions. However, when examining the seismic codes that have been in effect over the last 50 years, none of the regulations permit the designer to deviate from the 135-degree hook design.

The presence of diagonal members or diagonal axes in the floor plans of the buildings resulted in shear damage to the beams and the joints where these beams were connected to columns. Using non-parallel axes at the design stage, although not considered as an irregularity in the design codes, caused shear failure in the structural elements (Doğan et al. 2021). Similarly, the presence of discontinuous beams and incomplete frames in the building systems, despite being designed with ductility in mind, resulted in significant damage to the reinforced concrete elements. The percentage distribution of irregularities observed in the examined building cluster, based on the total number of buildings, is presented in Fig. 18.

Based on the identified deficiencies and irregularities, an analysis model was developed for the damaged buildings, incorporating common characteristics of the structural system and elements. Analyzes were carried out on SAP2000 (2020).

The building stock examined during field investigations includes buildings from single storey to 15 storeys. It has been observed that the number of 4-storey buildings is the majority among the 540 buildings whose floor distribution is presented proportionally in Fig. 19. Hence, the models were designed as four-story structures with all columns measuring 300×500 mm, beams measuring 250×500 mm, and RC wall thickness measuring 250 mm, ensuring geometric rigidity consistency. The building models consist of one ground floor with a height of 3.5 m and three typical floors with a height of 2.5 m each, resulting in a total building height of 11 m. To compare the damage and behaviour between different analysis approaches, a second analysis model with the same geometry and structural system properties but fully compliant with the section design principles specified in TBEC2018 was also devised. The floor plan of the utilized building models for analysis is shown in Fig. 20. The analysis models include short columns, diagonal axes, soft stories, discontinuous beams, and plan irregularities. Among the generated models, the one adhering to TBEC2018 in terms of section design and material strengths was referred to as the Confined High Material Grade (CHMG) model,
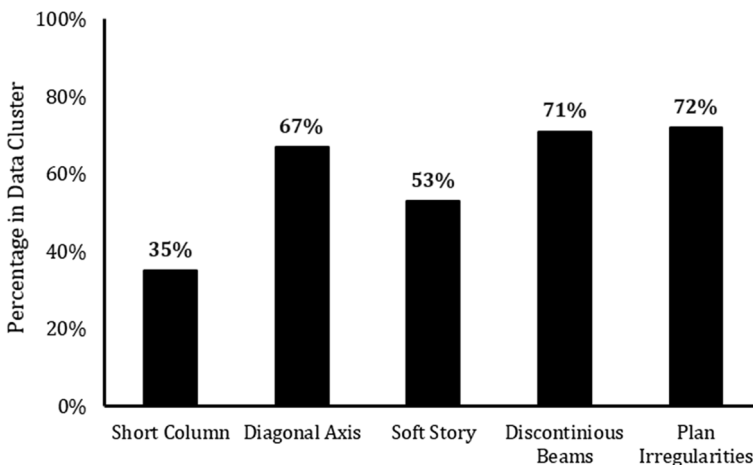

Fig. 18 The percentage distribution of ırregularities and deficiencies in the data cluster

Fig. 19 Proportional distribution of the examined buildings according to their number of stories
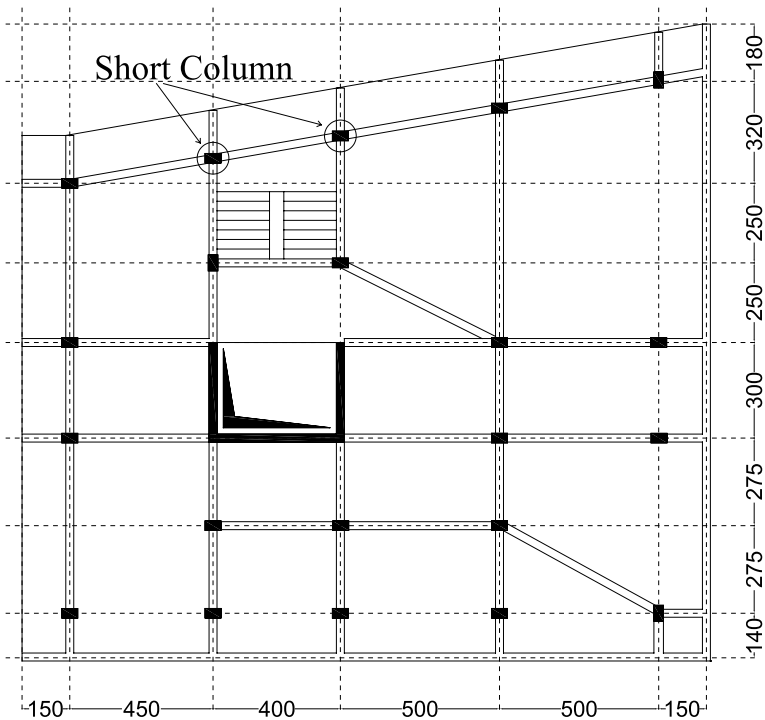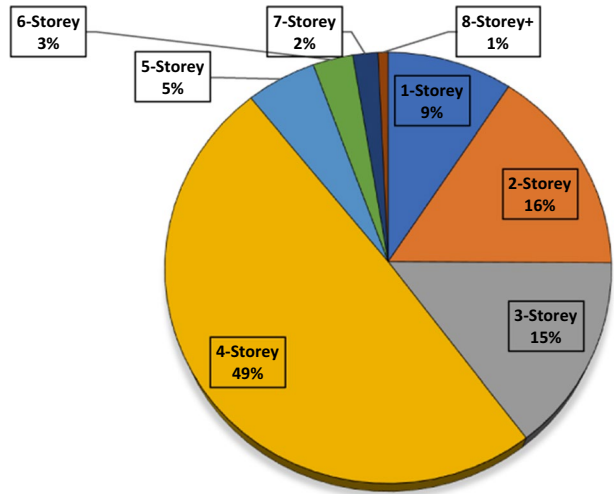

**Fig. 20** Floor plan of the analysis models (dimensions in cm)

while the model with insufficient confinement and low material strength according to the regulations given in TBEC2018 was labelled as the Unconfined Low Material Grade (ULMG) model.

The section designs of the CHMG model were carried out in accordance with the TS500 design standard and aligned with the requirements of TBEC2018. The gravitational loads used were obtained from TS498, while the response spectra generated for the coordinates of the stations provided in Table 1 were used for seismic loads (Turkish Standardization Institute 1987, 2000). The CHMG model has a concrete strength of 30 MPa and S420 reinforcement. In the ULMG model, the concrete strength is 16 MPa and S220 reinforcement is used. Since the geometries of the structural system elements are identical in both models, the difference in structural stiffness is governed by the material strengths and element designs. However, despite this, there is an approximate 0.1-s difference in the fundamental period between CHMG (with a period of 0.98 s) and ULMG (with a period of 1.07 s). This difference is consistent with the similarity in initial slopes of the capacity curves obtained from static pushover analyses conducted, as shown in Fig. 21, following the guidelines of ATC-40 (Council 1996).

Plastic hinges have been defined on the structural system elements as per the nonlinear analysis procedures. The adoption of cumulative plastic hinges was preferred to model the bending and shear damage of columns and beams, due to its capability to provide close results to experimental data, its frequent use in the literature, and its ability to expedite the analysis process (Inel and Ozmen 2006; Marante and Flórez-López 2003; Vafaei et al. 2020). The hysteresis behaviour model proposed by Pampanin et al. (2003) has been idealized as a bilinear hinge model to simulate the shear damage observed in beam-column connections, which was frequently observed during field inspections. In the beam-column connections, the beam ends were assumed to be rigidly connected to the column surfaces, and shear hinges were placed at the centre of the remaining height within the joint area. PMM hinges (Axial-Moment-Moment) were placed at the column ends, and shear hinges were placed at the midpoints of the spans. For RC walls, the PMM fibre hinge (Sap2000 2020) model was used, and shear hinges were defined at the midpoints of the walls. Nonlinear pushover and time history analyses were performed on the analysis models. The analysis results were compared in terms of energy dissipation capacity, ductility, and performance objectives, and overall behavioural differences were presented.

Due to the significant difference in material strengths and the brittle behaviour of unconfined elements, some elements experienced early capacity loss. As a result, the ULMG model was unable to reach the 0.01 roof displacement ratio. Although both models did not reach the commonly encountered 0.04 roof displacement ratio in pushover analyses, the CHMG model, with the aid of the Mander Confined Concrete Model, was able to achieve a value close to 0.03 roof displacement ratio (Krawinkler and Seneviratna 1998; Mander et al. 1988). When compared in terms of overall energy dissipation capacity, it can be

Fig. 21 Comparison of pushover curves
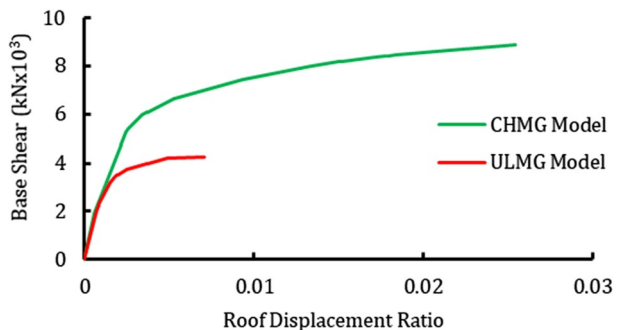
said that the model designed according to TBEC2018 principles is approximately 5 times superior.

Time History analysis was performed using the earthquake records obtained from stations 3141 and 3125, whose locations are shown in Fig. 3 and soil properties are presented in Table 1, for the studied region based on detailed field investigations. No scaling was applied to the earthquake records as the soil classes of the stations were generally similar to those of the examined buildings, and the stations were located within a 10 km radius of the studied region. The acceleration records used in the time history analysis were applied to the buildings, following the response spectra given in Fig. 4. Time history analyses were conducted using a total of 4 sets of input records obtained from 2 stations for the Pazarcık and Samandağ earthquakes. The input records applied to the building models sequentially to simulate successive ground motions. The analysis results were compared in Fig. 22 for the base shear and roof displacement data of each record set. Furthermore, the base shear-roof displacement ratio relationships were visualized in Fig. 23 as hysteresis curves for the time history analyses and compared with capacity curves.

The compared base shear and roof displacement ratios were evaluated for the weak direction of the building in both analysis models, which exhibit asymmetry and structural irregularities. The CHMG model, which has superior material strength and section properties, and is slightly stiffer in terms of structural fundamental period, experienced higher base shear forces. Similarly, due to the lack of confinement, the ULMG model, which is at a disadvantage, has achieved significantly lower roof displacement values. Similarly, the ULMG model, which is disadvantaged due to confinement effects, achieved significantly lower roof displacement values.

Based on the results of the time history analyses, the models exhibited similar behaviour to the pushover analysis results and formed plastic hinge formations as shown in Fig. 24. Due to its insufficient ductility, the ULMG model generated hysteresis loops close to the capacity curve and underwent mechanism behaviour with the formation of beam-column connection hinges and the failing of ground floor columns. On the other hand, CHMG, with its ductile design, achieved higher base shear and greater roof displacements in the time history analyses. After the elastic moment capacities of the beams were exceeded, the mechanism state was reached as a few ground-floor columns sustained damage. In terms of base shear force, CHMG had approximately twice the capacity, while in terms of roof displacement, it had approximately three times the capacity compared to ULMG. In CHMG,
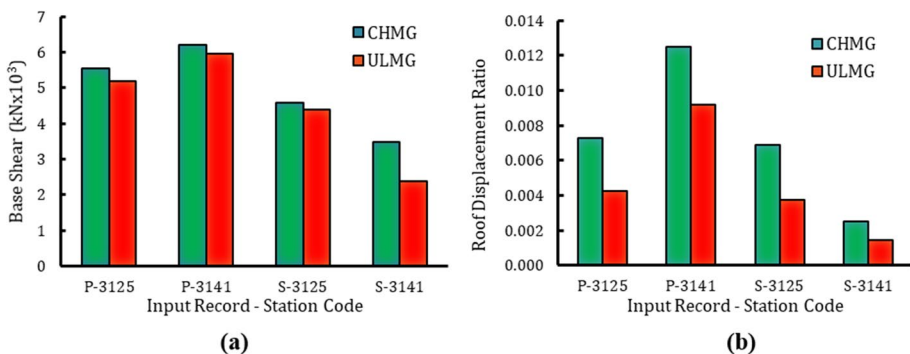

Fig. 22 Nonlinear time history analysis results: **a** Max. Base shears, **b** Max. Roof displacement ratios
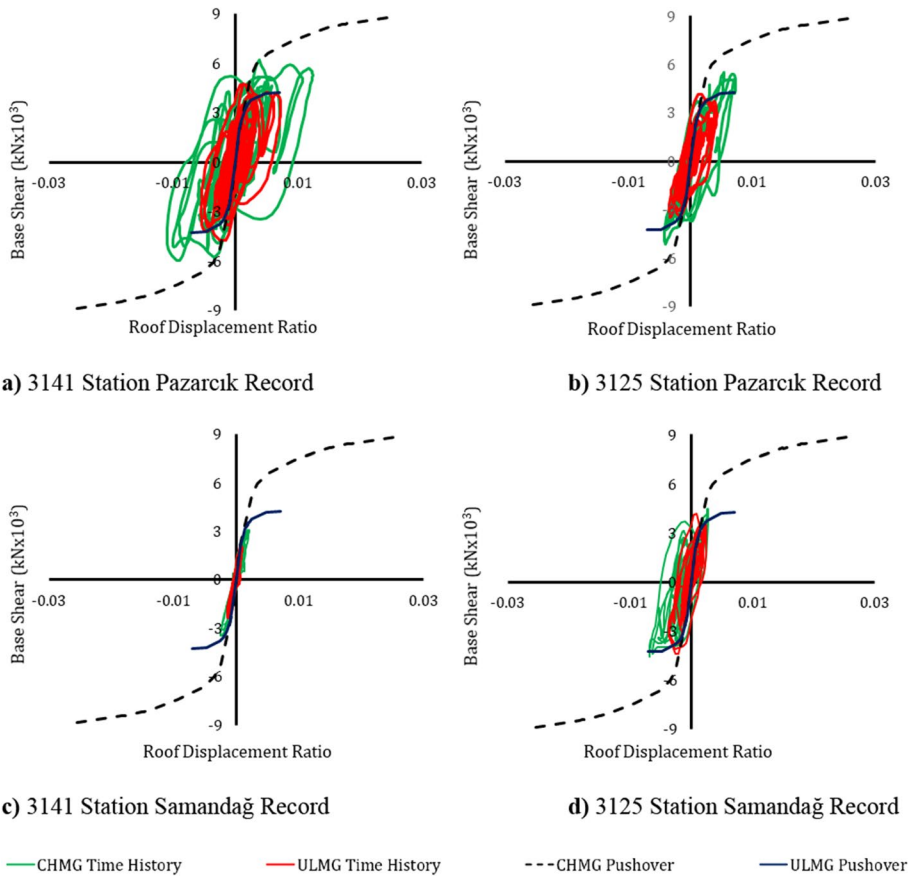
Fig. 23 Comparisons of hysteretic loop curves and capacity curves as a result of nonlinear analyzes

with input records obtained from station 3141, the analyses applied during the Pazarcık Earthquake resulted in initial-level yielding, followed by progressive damage and the formation of new hinges with the Samandağ earthquake. In contrast, in ULMG, all hinges were formed during the analysis of the Pazarcık Earthquake. Due to the lower acceleration values obtained from station 3141 for the Samandağ earthquake, advanced-level yielding was not observed. Although the models could not reach the accelerations that would lead to advanced deformations for the other three earthquake records, advanced-level hinge formations were observed mainly at the beam ends in the CHMG model, while in the ULMG model, plastic hinges were predominantly formed at the lower ends of the columns.

5 Analysıs results

The nonlinear analyses of the CHMG and ULMG models, designed based on the data obtained from field observations, revealed significant differences in their overall base shear, displacement, and energy dissipation capacities due to variations in material strengths, confinement effects, and connection stiffness. Additionally, the seismic performance of the
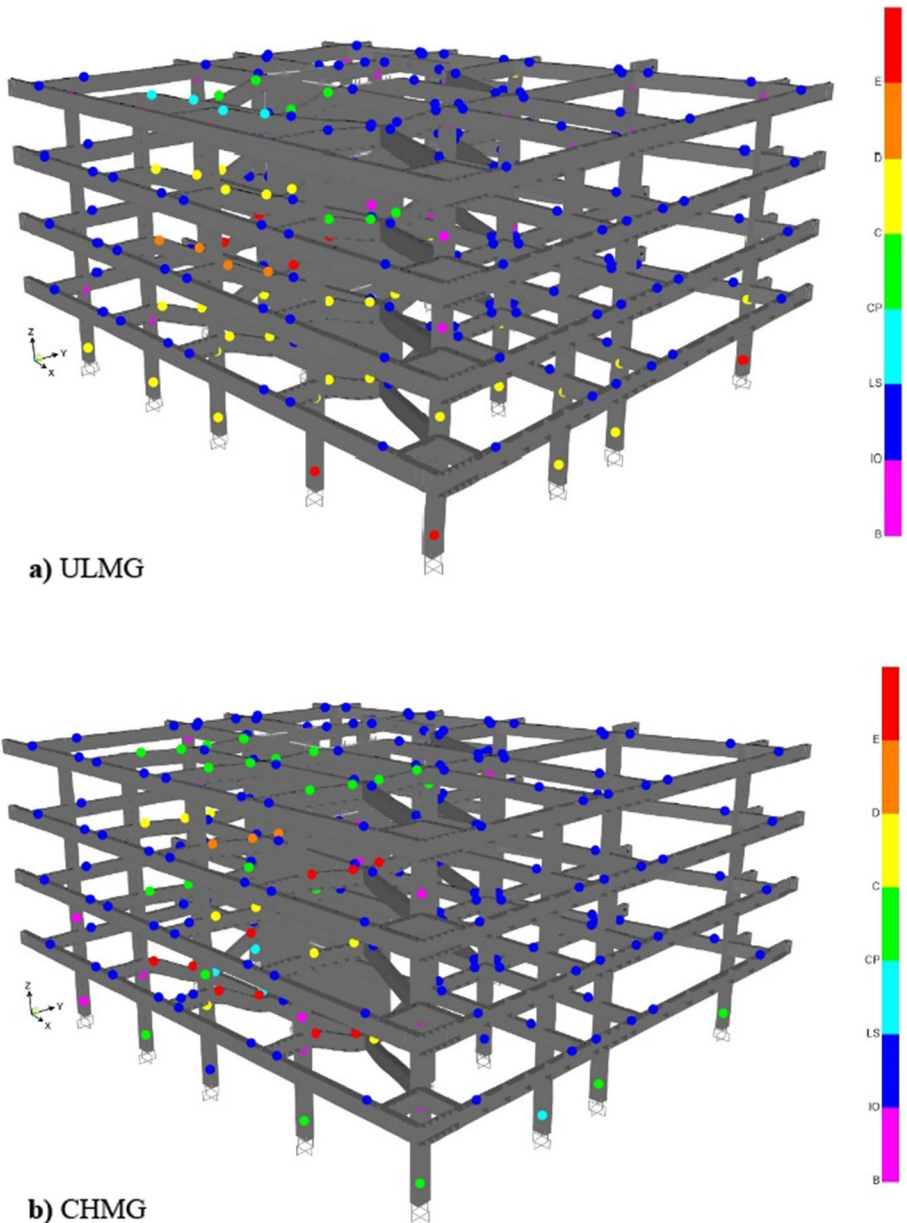
a) ULMG

b) CHMG

Fig. 24 Hinge formation at the end of the time history analysis for 3141 Pazarcık record

buildings was evaluated according to TBEC2018 criteria. The investigations revealed that the ULMG model transitioned to the collapse state without achieving the Life Safety (LS) performance level. On the other hand, despite having identical geometry with the ULMG model, the CHMG model, which had higher material quality and effective confinement reinforcement, met its performance point. The performance points of the structures are

presented in Fig. 25 in the form of Acceleration-Displacement Response Spectra (ADRS). Furthermore, despite the low difference in structural periods, indicating close proximity in terms of stiffness within the linear elastic range, errors during construction (confinement) led to insufficient ductility behaviour of the ULMG model, resulting in early capacity loss and transitioning to the mechanism state. Here, despite incorporating structural irregularities and design errors, CHMG achieves the performance objective with a roof displacement ratio capacity of 0.026. However, the ULMG model falls behind the performance objective with a roof displacement ratio capacity of 0.007. The analyses conducted reveal that with sufficient material quality and proper implementation of confinement reinforcement, the roof displacement ratio can be increased by approximately three times.

During the field investigations, when the analysis results were evaluated according to the method proposed by Ilki et al., the ULMG model would be classified as heavily damaged because it has at least one D type damage in its columns (core crushing, rebar buckling or CP and C for analysis result). Similarly, the CHMG model would also be considered heavily damaged according to this method, as it has more than three C type damages (cover spalling or LS for analysis result). After the completion of the assessments in the disaster-affected area, the heavily damaged buildings were decided to be demolished. However, with the determination of material properties through sampling from the structural systems of these buildings, followed by detailed nonlinear analyses for performance evaluation, the buildings can be repaired or strengthened. For decision-making regarding demolition or strengthening based on detailed analysis outputs, Park and Ang introduced the *"Damage Index" (DI_{PA})*, which was later developed as DI_{BB} by Bozorgna and Bertero. According to this index presented in Eq. 1, if $DI_{BB} > 0.5$, the buildings are classified as "Irreparable Damage" and require demolition. If this value is less than 0.5, the building can be strengthened (Bozorgnia and Bertero 2003; Park and Ang 1985).

$$\mathrm{DI}_{BB} = \frac{(1-\alpha)(\mu-1)}{\mu_{mon}-1} + \alpha\frac{E_H}{E_{mon}} \tag{1}$$

Here, α is constant at 0.3 for ULMG and CHMG, E_H represents the energy consumed by hysteretic loading, E_{mon} represents the energy capacity obtained from static pushover analysis, μ represents the ratio of maximum roof displacement in hysteretic loading to the elastic limit displacement in static pushover analysis, and μ_{mon} represents the ductility coefficient obtained
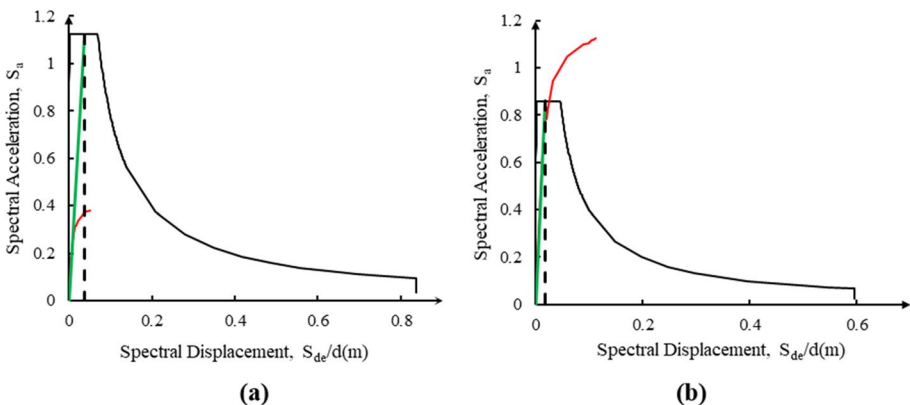

Fig. 25 Spectral performance comparison of **a** ULMG, **b** CHMG

from static pushover analysis. Table 3 presents the calculated DI_{BB} indices for ULMG and CHMG. The DI_{BB} values were computed using the results obtained from nonlinear analyses applied to the analysis models that require a decision for demolition according to the methods proposed by Ilki et al. For ULMG, the calculated DI_{BB} value exceeded the threshold for demolition. However, for CHMG, the calculated DI_{BB} value is less than 0.5, indicating that the building can be strengthened according to this method.

6 Conclusıon

This study presents the findings of field investigations conducted after the Kahramanmaraş earthquakes on February 6th. According to the examinations, it has been observed that the damages and collapses leading to loss of life in the region are generally due to the presence of multiple structural errors together.

In Hatay, the majority of residential buildings, regardless of the size of the foundation area, have cantilever projections on all possible facades. A significant percentage of these projections have incomplete beam frames, resulting in structurally irregular axes. There are numerous buildings with structural systems consisting of moment-resisting frames, which incorporate design details that lead to damage in short columns. Many buildings with soft stories and weak stories, as defined in TBEC2018, have partially or completely collapsed. In addition to these errors and irregularities, it has been observed that the main cause of severe damage in the heavily affected structures is insufficient material quality and inadequate reinforcement detailing. In buildings that were constructed before the implementation of modern seismic codes, low-strength reinforcement was used, and inappropriate aggregates such as river sand and sea sand, which adversely affect concrete strength, were also found. The differences in analysis results obtained from models developed with these defects support the high level of damage and collapse observed. The CHMG model, which incorporates various structural irregularities such as soft stories and short columns but possesses adequate reinforcement detailing and high material strength, was found to meet the performance objective according to the results of time history analyses. On the other hand, the ULMG model, which lacks sufficient material quality and reinforcement detailing, failed to ensure life safety. Thus, it can be concluded that the primary factors contributing to the loss of life after the earthquake were inadequate material quality and insufficient reinforcement detailing.

In the investigated disaster area, the most common causes of destruction found in collapsed or newly constructed buildings are: column-beam joint mechanisms, weak column-strong beam connections, weak/soft story irregularities, and shear damage in vertical structural elements.

In the study presented by Doğan et al., the rapid visual screening methods examined for determining the risk status of buildings and prioritizing inspections have been observed to have the potential for success (Doğan et al. 2021). However, the post-earthquake damage assessment method proposed by Ilki et al. has been noted to be a conservative approach for ductile buildings (Ilki et al. 2021). This situation has been exemplified through the analysis

Table 3 Calculated DI_{BB} for both CLMG and ULMG

Model	E_H	E_{mon}	μ	μ_{mon}	DI_{BB}
ULMG	90.89874	91.17136	4.910213	4.75972	1.027
CHMG	697.099	1360.751	3.63045	7.3759	0.4415

model results by Park and Ang, modified by Bozorgna and Bertero, and presented with the "Damage Index" (Mander et al. 1988; Bozorgnia and Bertero 2003).

The analysis results have shown that even though a building may have structural irregularities such as short columns, soft stories, cantilever beams, and discontinuous/diagonal axes, if it is constructed in accordance with modern earthquake codes and design standards, and its construction stages are properly monitored to ensure compliance with the approved design, it will achieve the desired performance (CHMG). The building will exhibit ductile behaviour, dissipating seismic energy and providing occupants with sufficient time to evacuate. On the other hand, in a structure like ULMG, it was observed that the maximum roof displacements exhibited by the building models in the pushover analysis were governed by shear hinges. The ULMG model was not designed to be ductile. Therefore, shear hinges were formed and limited the expected roof displacements. Hence, the sudden damage to ground floor columns in the early seconds of an earthquake triggers a chain of damage progression, ultimately leading to the building's collapse in a short period of time.

The construction errors observed in buildings designed for ductile behaviour have resulted in severe damage. Moreover, these buildings were constructed when modern regulations were in effect. This unacceptable situation can be attributed to a lack of construction supervision and management. In this regard, it has become crucial to address the necessity of stricter legal measures to govern construction inspections. Despite being structurally robust according to their designs, many buildings have suffered collapse due to the lack of proper inspection.

The clearing of debris from collapsed buildings and the detailed analysis of the remaining structures will follow the aftermath of the earthquakes. The field inspections and analyses conducted for this research paper serve as an initial step for future investigations. Subsequently, by creating structural system surveys and damage surveys for the standing buildings, modal vibration measurements can be conducted on an actual building that has experienced the earthquake, allowing for the determination of modal parameters associated with the damaged state. Future research, focusing on comparing these parameters with the results of performance analyses conducted using structural system models, will contribute significantly to the literature.

Declarations

References

Achs G, Adam C (2012) Rapid seismic evaluation of historic brick-masonry buildings in Vienna (Austria) based on visual screening. Bull Earthq Eng 10:1833–1856

Ambraseys N, Jackson J (1998) Faulting associated with historical and recent earthquakes in the Eastern Mediterranean region. Geophys J Int 133(2):390–406

Ansal A et al (2003) Adapazarı ve Gölcük için mikrobölgeleme çalışmaları. *Beşinci Ulusal Deprem Mühendisliği Konferansı, İstanbul,* pp 1–14

Arpat E, Şaroğlu F (1972) The East Anatolian fault system; thoughts on its development. Bull Miner Res Explor 78(78):1–12

Arpat E (1971) 22 mayıs 1971 Bingöl Depremi; ölü Deniz fay sisteminin Karlıova ilçesi ile Hazar Gölü arasındaki bölümü (ön rapor). MTA Enst. Rap

Arslan M, Korkmaz HH (2007) What is to be learned from damage and failure of reinforced concrete structures during recent earthquakes in Turkey? Eng Fail Anal 14(1):1–22

Ates S, Kahya V, Yurdakul M, Adanur S (2013) Damages on reinforced concrete buildings due to consecutive earthquakes in Van. Soil Dyn Earthq Eng 53:109–118

Ateş R, Bayülke N (1977) Mart 1977 Palu Elazığ Depremi. *Deprem Araştırma Daire Başkanlığı, Ankara*.

Barka A, Kadinsky-Cade K (1988) Strike-slip fault geometry in Turkey and its influence on earthquake activity. Tectonics 7(3):663–684

Bayraktar A, Altunişik AC, Pehlivan M (2013) Performance and damages of reinforced concrete buildings during the October 23 and November 9, 2011 Van, Turkey, earthquakes. Soil Dyn Earthq Eng 53:49–72

Bektaş N, Kegyes-Brassai O (2023) Development in fuzzy logic-based rapid visual screening method for seismic vulnerability assessment of buildings. Geosciences 13(1):6

Bhalkikar A, Kumar RP (2021) A comparative study of different rapid visual survey methods used for seismic assessment of existing buildings. In Structures, vol 29. Elsevier, pp 1847–1860

Bozorgnia Y, Bertero VV (2003) Damage spectra: characteristics and applications to seismic risk reduction. J Struct Eng 129(10):1330–1340

Çağatay İH (2005) Experimental evaluation of buildings damaged in recent earthquakes in Turkey. Eng Fail Anal 12(3):440–452

Council A (1996) Seismic evaluation and retrofit of concrete buildings Report No ATC-40. In: SSC 96-01: ATC-40, vol 1

DEMP (2018) Seismic Hazard maps interactive web application. Disaster and Emergency Management Presidency, Ankara

Demirel IO, Yakut A, Binici B (2022) Seismic performance of mid-rise reinforced concrete buildings in Izmir Bayrakli after the 2020 Samos earthquake. Eng Fail Anal 137:106277

Demirtaş R, Yılmaz R (1996) Seismotectonics of Türkiye: preliminary approach to earthquake forecasting based on long-term variations in seismic activity and present seiemicity. Republic of Türkiye, Ministry of Public Works and Settlement

Doğan TP, Kızılkula T, Mohammadi M, Erkan İ, Kabaş HT, Arslan M (2021) A comparative study on the rapid seismic evaluation methods of reinforced concrete buildings. Int J Disaster Risk Reduct 56:102143

Doğangün A (2004) Performance of reinforced concrete buildings during the May 1, 2003 Bingöl Earthquake in Turkey. Eng Struct 26(6):841–856

Duman TY, Emre Ö (2013) The East Anatolian Fault: geometry, segmentation and jog characteristics. Geol Soc Lond Spec Publ 372(1):495–529

Erdil B, Ceylan H (2019) A detailed comparison of preliminary seismic vulnerability assessment methods for RC buildings. Iran J Sci Technol Trans Civ Eng 43(4):711–725

FEMA-154 (2017) Rapid visual screening of buildings for potential seismic hazards: a handbook. Government Printing Office

Harirchian E, Lahmer T (2020) Developing a hierarchical type-2 fuzzy logic model to improve rapid evaluation of earthquake hazard safety of existing buildings. In: Structures, vol 28. Elsevier, pp 1384–1399

Haryanto Y, Hu H-T, Han AL, Hidayat BA, Widyaningrum A, Yulianita PE (2020) Seismic vulnerability assessment using rapid visual screening: case study of educational facility buildings of Jenderal Soedirman University, Indonesia. Civ Eng Dimens 22(1):13–21

Ilki A, Halici O, Comert M, Demir C (2021) The modified post-earthquake damage assessment methodology for TCIP (TCIP-DAM-2020). In: Advances in assessment and modeling of earthquake loss. Springer International Publishing, Cham, pp 85–107

Inel M, Ozmen HB (2006) Effects of plastic hinge properties in nonlinear analysis of reinforced concrete buildings. Eng Struct 28(11):1494–1502

Kaplan H, Yilmaz S, Binici H, Yazar E, Çetinkaya N (2004) May 1, 2003 Turkey—Bingöl earthquake: damage in reinforced concrete structures. Eng Fail Anal 11(3):279–291

Kirac N, Dogan M, Ozbasaran H (2011) Failure of weak-storey during earthquakes. Eng Fail Anal 18(2):572–581

Krawinkler H, Seneviratna G (1998) Pros and cons of a pushover analysis of seismic performance evaluation. Eng Struct 20(4–6):452–464

Mander JB, Priestley MJ, Park R (1988) Theoretical stress-strain model for confined concrete. J Struct Eng 114(8):1804–1826

Marante ME, Flórez-López J (2003) Three-dimensional analysis of reinforced concrete frames based on lumped damage mechanics. Int J Solids Struct 40(19):5109–5123

McKenzie D (1972) Active tectonics of the Mediterranean region. Geophys J Int 30(2):109–185

McKenzie D (1978) Active tectonics of the Alpine—Himalayan belt: the Aegean Sea and surrounding regions. Geophys J Int 55(1):217–254

Nanda R, Majhi D (2013) Review on rapid seismic vulnerability assessment for bulk of buildings. J Inst Eng India Ser A 94:187–197

Pampanin S, Magenes G, Carr A (2003) Modelling of shear hinge mechanism in poorly detailed RC beam-column joints. Athens, Greece: fib 2003 Symposium "Concrete Structures in Seismic Regions", May 2003. Paper n.171

Park Y-J, Ang AH-S (1985) Mechanistic seismic damage model for reinforced concrete. J Struct Eng 111(4):722–739

TS500, Requirements for Design and Construction of Reinforced Concrete Structures, Ankara/Türkiye, 2000.

Sap2000 v22 (2020) https://www.csiamerica.com/

Şaroğlu F, Emre Ö, Boray A (1987) Türkiye'nin diri fayları ve depremsellikleri. MTA. Rap, vol 394

Şengör A, Görür N, Şaroğlu F (1985) Strike-slip faulting and related basin formation in zones of tectonic escape: Turkey as a case study, The Society of Economic Paleontologist s and Mineralogists, 227-264

Seymen İ, Aydin A (1972) The Bingöl earthquake fault and its relation to the North Anatolian fault zone. Bull Miner Res Explor 79(79):8–12

Sezen H, Whittaker A, Elwood K, Mosalam K (2003) Performance of reinforced concrete buildings during the August 17, 1999 Kocaeli, Turkey earthquake, and seismic design and construction practise in Turkey. Eng Struct 25(1):103–114

Standard B (2005) Eurocode 8: design of structures for earthquake resistance. Part 1:1998–2001

TBEC2018 (2018) Turkish Building Earthquake Code 2018. (Accessed)

Tapan M, Comert M, Demir C, Sayan Y, Orakcal K, Ilki A (2013) Failures of structures during the October 23, 2011 Tabanlı (Van) and November 9, 2011 Edremit (Van) earthquakes in Turkey. Eng Fail Anal 34:606–628

Tesfamariam S, Saatcioglu M (2008) Risk-based seismic evaluation of reinforced concrete buildings. Earthq Spectra 24(3):795–821

Vafaei M, Alih SC, Fallah A (2020) The accuracy of the lumped plasticity model for estimating nonlinear behavior of reinforced concrete frames under gradually increasing vertical loads. Struct Concr 21(1):65–80

Yakut A (2004) Preliminary seismic performance assessment procedure for existing RC buildings. Eng Struct 26(10):1447–1461

Yakut A et al (2021) Performance of structures in İzmir after the Samos island earthquake. Bull Earthq Eng 1–26

Yüksel İ (2008) Betonarme Binalarin Deprem Sonrasi Acil Hasar Değerlendirmeleri. Erciyes Üniversitesi Fen Bilimleri Enstitüsü Fen Bilimleri Dergisi 24(1):260–276